

Material and energy balance calculations for commercial production of whole neem fruit powder using particle-size distribution and energy models

Sonali Tajane¹, Praful Dadhe¹, Krishna Kanth Chole¹, Sachin Mandavgane^{1,*} and Sayaji Mehetre²

¹Department of Chemical Engineering, Visvesvaraya National Institute of Technology, South Ambazari Road, Nagpur 440 010, India

²Nuclear Agriculture and Biotechnology Division, Bhabha Atomic Research Centre, Mumbai 400 085, India

Neem-based pesticides are well known to reduce agriculture pollution. It was earlier found that free-flowing fine powder of whole dry neem fruits (called PNF-powder neem formulation) of size range 300 μm to 390 μm , i.e. (-44 + 60 mesh) was the optimum size range. Azadirachtin which is a key ingredient of neem is quite stable in PNF. This article delineates material and energy balance to produce 1 tonne of PNF on a commercial level by using hammer mill. The particle size distribution models and classical energy consumption models were used to fit the experimental data generated by changing the hammer mill screen.

Keywords: Co-grinding, energy, hammer mill, particle-size distribution, whole neem fruit.

INTENSIVE use of chemicals for agricultural purposes degrades water, soil and air, and is thus one of the main causes of pollution. To overcome this problem, suitable natural (organic) materials can be used as insecticides and pesticides. In this regard, neem (*Azadirachta indica*) is considered a potential alternative for most agricultural applications¹. However, extraction and separation of Aza, the principal component in neem, is a costly process; in addition, the amount of Aza extracted/separated is low. Other natural products of neem such as neem oil, neem kernel cake, and neem leaves powder are available in the market for direct application. Among these, neem kernel has the highest percentage of Aza. Neem oil is obtained from the kernel by cold pressing, and the remaining solid waste is called kernel cake or neem cake. Since the aforementioned products are subjected to unit operations such as depulping and decorting, the percentage of Aza obtained from these products is low, which makes them

less effective in agricultural applications. Besides, the dry pulp and shell, which contain a reasonable amount of Aza, are not utilized in these processes. Therefore, in this study, the whole dry neem fruits are ground into fine powder without extracting oil, which make it an effective pesticide. The powder thus obtained has a large surface area and shows better biological activity owing to the presence of limonoids (e.g. salannin and nimbolide), which also helps to increase the shelf life of the products². To obtain a free-flowing fine powder of oil seed/fruits, whole neem fruits were co-ground with an inert material (dolomite). Dolomite is an anhydrous carbonate mineral composed of calcium magnesium carbonate [$\text{CaMg}(\text{CO}_3)_2$]. The materials obtained also act as a source of essential nutrients (i.e. calcium and magnesium), which help the growth of plants^{3,4}. Dolomite is cheap, easily available, and helps to neutralize the pH of acidic soil. Hammer mill is identified to be the most suitable equipment for grinding dry neem fruits. Size reduction is an energy intensive operation. It is desirable that the product thus formed should have uniform distribution of desired particle size. Different models to correlate comminution parameters have been reported previously. For example, Rosin–Rammner–Bennett (RRB), Gaudin–Schumann (GS) models and log–normal distribution were used to express particle-size distribution and size parameter of powders of mango-ginger⁵, coriander⁶ and cork⁷. Mohd Rozallil⁸ studied energy consumption specifically during grinding of peanuts in an ultra-high-speed grinding machine. In another study, Miao *et al.*⁹ reported on the energy requirement for size reduction of biomass.

In this work, particle size, particle size distribution, and energy consumption models were applied to the experimental data obtained by co-grinding dry whole neem fruit with dolomite in a hammer mill. The best fit model was used to calculate energy and material required for production of PNF on commercial level having uniform size of desired particle size-range.

*For correspondence. (e-mail: mandavgane@gmail.com)



Figure 1. PNF of different size sample obtained from hammer mill HM 1.2, HM 0.8 and HM 0.4.

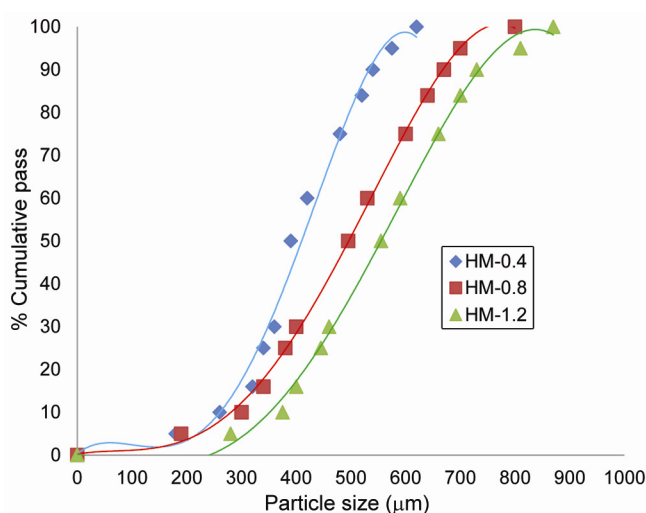


Figure 2. Cumulative mass percentage versus size plot of PNF obtained from three different hammer mill screens.

Materials and methods

Materials and synthesis of powder neem formulation¹⁰

Dry neem fruits and dolomite were purchased from a local market in Nagpur (India). Whole dry neem fruits were washed, cleaned and dried (pre-treatment). The dried fruits were then pulverized with powder dolomite in a hammer mill (RPM-9000, HP-2 Shubh Micro Baby Pulverizer, in Mumbai, India) with 1:1 ratio of dry whole neem fruit (average size of 10.122 mm) to dolomite powder (size ≤ 0.106 mm). Whole dry neem fruit (with 0.28% of Aza) and dolomite are fed with equal percentage to the hammer mill so that during grinding of the whole neem fruit, the oil released gets easily absorbed by dolomite and results into free flowing powder¹⁰. The hammer mill hammers are swing type, and the detailed set-up was similar to that reported by Shashidhar⁶. However, in this study, different classifying screens, namely, HM 1.2, HM 0.8 and HM 0.4, were used to obtain three different particle size samples of powder neem formulation (PNF) (Figure 1).

Sieve analysis

Sieve analysis of PNF obtained from each screen was performed in a laboratory sieve shaker using the British

standard sieves (make Sethi standard test sieve Mumbai). The sieves were arranged such that the large aperture size sieve was at the top and the small aperture size sieve was at the bottom. Approximately 100 g of PNF was loaded on the top screen, and the sieves were shaken for about 20 min. The material retained on each screen was weighed, and the mass fraction determined. Each experiment was repeated three times, and the average values were used for calculation. Figure 2 shows the cumulative plot of particle-size distributions of PNF obtained from three different screens. It was observed from the cumulative plot that the powder (PNF) obtained from HM 1.2 is coarser as compared to HM 0.8 and HM 0.4. This is because of the punched plate opening size (hammer mill screen) which controls the size of PNF. Hammer mill screen with HM 1.2 yielded coarser product as the screen opening was around 1.2 mm as compared to HM 0.8 (having 0.8 mm screen opening size) and HM 0.4 (having 0.4 mm screen opening size). Hence a finer size of PNF was obtained with hammer mill HM 0.4.

Mathematical models for particle-size distributions

Particle-size distribution of the powder samples can be modelled by various mathematical models, as discussed earlier⁷. In this work, the Rosin–Rammler–Bennett^{11,12}, Gaudin–Schumann^{13,14} equations and log-normal distribution were used to model the particle-size-distribution data of PNF, as these models are particularly suited to represent powder made by grinding, milling and crushing operations. The mathematical functions used to describe the size-distribution data are as follows.

Rosin–Rammler–Bennett (RRB) equation

$$Y = 1 - \exp \left[\left(\frac{-X}{X_R} \right)^{nR} \right] \quad (1)$$

Gaudin–Schumann (GS) equation

$$Y = \left(\frac{X}{X_G} \right)^{nG}, \quad (2)$$

where Y is the cumulative mass fraction (%), x the particle size, x_R and x_G are the size parameters of RRB

Table 1. Cutoff diameter for the three different PNF samples obtained from hammer mill

Cutoff diameter (μm) at different cumulative undersize mass, %	Hammer mill screen		
	HM 1.2	HM 0.8	HM 0.4
x_5	280	190	180
x_{10}	375	300	260
x_{16}	400	340	320
x_{25}	445	380	340
x_{30}	460	400	360
x_{50}	555	495	390
x_{60}	590	530	420
x_{75}	660	600	480
x_{84}	700	640	520
x_{90}	730	670	540
x_{95}	810	700	575

Table 2. Formula for calculating different size parameters from literature

Parameter	Formula	Reference
Size guide number	$S_{gn} = x_{50}$	8
Effective size	$E_s = x_{10}$	19
Uniformity index	$U_i = \frac{100 * x_5}{x_{95}}$	18
Coefficient of uniformity	$C_u = \frac{x_{60}}{x_{10}}$	19
Coefficient of gradation	$C_g = \frac{x_{30}^2}{x_{10} * x_{60}}$	19
Inclusive graphic skewness	$I_{gs} = \left(\frac{x_{16} + x_{84} - 2 * x_{50}}{2 * (x_{84} - x_{16})} \right) + \left(\frac{x_5 + x_{95} + x_{95} - 2 * x_{50}}{2 * (x_{95} - x_5)} \right)$	13
Graphics kurtosis	$G_k = \frac{x_{95} - x_5}{2.44(x_{75} - x_{25})}$	13
Graphic mean	$G_m = \left(\frac{x_{16} + x_{50} + x_{84}}{3} \right)$	13
Inclusive graphics standard deviation	$I_{gsd} = \left(\frac{x_{84} - x_{16}}{4} \right) + \left(\frac{x_{95} - x_{50}}{6.6} \right)$	13
Standard geometric deviation	$GSD1 = \frac{x_{84}}{x_{50}}; GSD2 = \frac{x_{50}}{x_{16}}; GSD12 = \left(\frac{x_{84}}{x_{16}} \right) 0.5$	20
Mass relative span	$M_{rs} = (x_{90} - x_{10})/x_{50}$	21

and GS respectively, and n_R and n_G are the distribution parameters of RRB and GS respectively.

Log-normal distribution

Another function which has been in wide use for the analysis of population distribution is the log-normal distribution function which is as below

$$dY = \xi \exp \left[\log_e 2 \left(\frac{x}{x_m} \right) \right] dx, \tag{3}$$

where b is steepness constant

$$b = \frac{1}{(2 \ln^2 \sigma_g)}, \tag{4}$$

σ_g is the size ratio corresponding to the 84% cumulative undersize mass fraction (x_{84}) and the 50% cumulative undersize mass fraction (x_{50})

$$\xi = \left(\frac{b}{\pi} \right)^{0.5} \frac{\exp(-1/4b)}{x_m}, \tag{5}$$

x_m represents the mode of the distribution which is equal to cX_{50} .

$$c = \exp \left(-\frac{1}{2b} \right). \tag{6}$$

Statistical analysis

To evaluate the goodness of fit, statistical parameters such as coefficient of determination (R^2), residual sum

Table 3. Estimated values of statistical and model parameters of RRB and GS models

	RRB model					GS model				
	Statistical parameters			Model parameters		Statistical parameters			Model parameters	
Hammer mill sieve	R^2	RSS	RSME	x_R	n_R	R^2	RSS	RSME	x_G	n_G
HM 1.2	0.890	3.177	0.564	567.2	2.816	0.883	1.619	0.424	567.2	2.81
HM 0.8	0.956	2.447	0.495	519.66	2.590	0.920	2.057	0.478	519.66	2.59
HM 0.4	0.964	4.423	0.665	464.83	2.390	0.883	5.556	0.754	464.83	2.39

Table 4. Numerical values of log-normal distribution parameters and statistical values

Parameter	Hammer mill screen		
	HM 0.8	HM 0.8	HM 0.4
Log-normal distribution parameter			
Mean	545.91	476.82	381
Standard deviation	167.68	167.21	113.96
R^2	0.883	0.910	0.789
84% size (μm)	700	640	390
50% (μm)	555	495	390
σ_y	1.261	1.292	1.333
b	9.29	7.617	6.0520
c	0.9476	0.936	0.9207
x_m	525.918	463.32	359.0743
Statistical parameters			
R^2	0.883	0.910	0.789
RSS	0.281	2.942	5.891
RSME	0.468	0.532	0.910

square (RSS), and root-mean-square error (RMSE) were determined. The best fit was chosen based on the R^2 value, which indicates the linear relationship between the experimental and predicted values

$$RSS = \sum_{i=1}^N (Y_{\text{exp},i} - Y_{\text{pre},i})^2, \tag{7}$$

$$RSME = \sqrt{\frac{\sum_{i=1}^N (Y_{\text{exp},i} - Y_{\text{pre},i})^2}{N}}, \tag{8}$$

where Y_{exp} and Y_{pre} are the experimental and predicted values of cumulative mass fraction expressed in percentage at any observation i respectively, and N is the total number of observations.

Size and distribution parameters

The particle-size distribution of PNF can also be expressed in terms of size-related parameters and distribution-related parameters⁶. Table 1 presents the particle-size distribution of PNF corresponding to the cumulative mass fraction.

The size and distribution parameter formulas used in the article are listed in Table 2. Size-related parameters are size guide number, effective size and graphic mean. Size guide number calculates mean particle size. Effective size is the size corresponding to 10% of cumulative mass (i.e. particle size corresponding to x_{10}). Folk and Ward¹³ proposed an empirical expression to calculate graphic mean. Distribution-related parameters are uniformity index, coefficient of uniformity, coefficient of gradation, including graphic skewness, graphic kurtosis, graphic standard deviation, standard geometric deviation and mass-relative span. Uniformity index gives the range of particle size; coefficient of uniformity (Cu) confirms whether the mass is well graded. So when Cu is greater than 4 to 6, it is understood as well graded and when Cu is less than 4, it is considered to be poorly graded or uniformly graded; coefficient of gradation indicates the uniformity of mass. Inclusive graphic skewness measures the degree of symmetry in the variable distribution and sign of skewness indicates whether the long tail is on the right or left side.

Inclusive graphic kurtosis measures the degree of flatness or peakiness in a given mass distribution. Geometric standard deviation measures the spread of values about the distributions. Separate expressions to measure geometric standard deviation for the following mass-fraction

regions are listed in Table 3: high region (between x_{84} and x_{50}), low region (between x_{50} and x_{16}) and total region (between x_{84} and x_{16}).

Mathematical functions for grinding energy calculation

The energy laws for size reduction were used to determine the correlation between power required for size reduction and size obtained in three different sieves of hammer mill. From the sieve analysis of PNF, the mass mean diameter, volume mean diameter and volume surface mean diameter were determined for each sample.

According to Rittinger's law, the work required in crushing is proportional to the new surface created. This is equivalent to the statement that the crushing efficiency is constant and, for a given machine and material, is independent of the size of feed and product. If the sphericities F_a (before size reduction) and F_b (after size reduction) are assumed to be equal and the machine efficiency is constant, then Rittinger's law can be written as follows

$$E = K_R[(1/D_P) - (1/D_F)]. \quad (9)$$

According to Kick's law, the work required for crushing a given mass of material is constant for the same reduction ratio, that is, the ratio of the initial particle size to the final particle size

$$E = K_K \ln(D_F/D_P). \quad (10)$$

According to Bond's law, the work required to form particles of size D_P from a very large feed is proportional to the square root of the surface-to-volume ratio of the product

$$E = K_B[(1/\sqrt{D_{P80}}) - (1/\sqrt{D_{F80}})]. \quad (11)$$

The work index W_i , is defined as the gross energy required in kilowatt hours per tonne of feed to reduce a very large feed to such a size that 80% of the product passes through a 100- μm screen

$$K_B = \sqrt{100 \times 10^{-3}} W_i = 0.3162 W_i, \quad (12)$$

$$E = 0.3162 W_i \left(\frac{1}{\sqrt{D_{P80}}} - \frac{1}{\sqrt{D_{F80}}} \right), \quad (13)$$

where E is the specific energy required (kJ/km of dry neem fruit), D_F the initial diameter of dry neem fruit (mm), D_P the mass mean diameter of PNF (mm), K_R Rittinger's coefficient, K_K Kick's coefficient, K_B a constant

that depends on the type of machine and the material being crushed, D_{P80} the mean diameter corresponding to d_{80} (mm), and m is the mass flow rate (t/hour).

Results and discussion

Mathematical function for particle-size distribution

Experimental data were fitted to the linear form of RRB and GS models and are shown in Figures 3a and b respectively. The distribution and statistical parameters of log-normal distribution model are shown in Table 4. It was found that the data showed better fit to the RRB model ($R^2 = 0.890-0.964$) than the GS model ($R^2 = 0.883-0.920$) and log-normal distribution model ($R^2 = 0.789-0.912$). From Table 4, it is seen that the distribution parameter n_R decreases with a decrease in the sieve size of the hammer mill, indicating that the distribution of particle size was directly proportional to the sieve size of the hammer mill. The size parameter x_R also followed the same trend.

A correlation between RRB parameters x_R and n_R with hammer mill sieve size (H_{ss}) was developed by regression analysis.

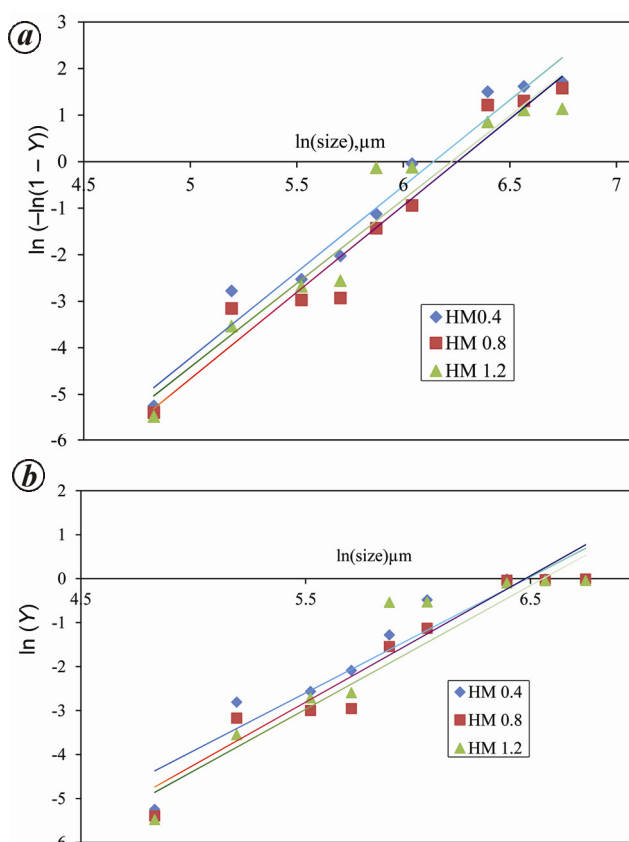


Figure 3. Particle-size distribution of PNF. a, RRB model; b, GS model.

Table 5. Size and distribution parameter for three different PNF samples obtained from hammer

Parameter	HM 1.2	HM 0.8	HM 0.4
Size related			
Size guide number	555	495	390
Effective size	375	300	260
Graphic mean	551.66	491.66	410
RRB sieve parameter	567.2	519.66	464.83
Distribution related			
Uniformity index (UI)	32.94	27.14	31.30
Coefficient of uniformity (Cu)	1.57	1.76	1.61
Coefficient of gradation (Cg)	0.95	1.00	1.186
Graphic kurtosis	1.08	0.95	1.156
Graphic skewness	0.00087	-0.11	0.11
Graphic standard deviation	161.36	152.27	109.84
Standard geometric deviation (GSD1)	1.26	1.29	1.33
Standard geometric deviation (GSD2)	1.38	1.45	1.21
Standard geometric deviation (GSD12)	1.32	1.37	1.27
Mass relative span	0.63	0.74	0.71

$$x_R = 127.9H_{ss} + 414.8, \tag{14}$$

$$n_R = 2.2e^{0.205 H_{ss}}. \tag{15}$$

The R^2 values for eqs (14) and (15) are 0.998 and 0.999 respectively. Similarly, by regression analysis, the relationship between average mass mean diameter (D_{mass}) and H_{ss} was established ($R^2 = 0.992$) as follows

$$D_{mass} = 45.14H_{ss} + 332.9 \text{ with } R^2 = 0.992. \tag{16}$$

Thiruparthihalli⁴ noted that n_R follows logarithmic equation, whereas x_R follows the power equation with H_{ss} . The distribution and statistical parameters of log-normal distribution model ($R^2 = 0.789-0.912$) are shown in Table 4.

Size and distribution parameters

The size-related parameters presented in Table 5 were calculated, among which size guide number (SGN), graphic mean and effective size decreased with decreasing H_{ss} . Uniformity index (UI) expresses the range of particle size. In this study, the value of UI was >20 and <60 for all three samples, which indicates even spreading of PNF. For skewness greater than 1 or less than -1 , the distribution is far from being symmetrical. The small positive value of skewness was obtained for PNF samples HM 0.4 and HM 1.2 (0.11 and 0.00087 respectively), indicating that these samples mostly had symmetrical distribution with slight asymmetry along a tail to the right side. By contrast, the PNF sample HM 0.8 had negative skewness (-0.11), which indicates slight asymmetrical distribution along a tail to the left side.

Kurtosis is a measure of degree of peakiness in variable distribution. The kurtosis values of each sample were greater than 1, indicating high degree of peakiness (i.e. leptokurtic distribution). Coefficient of uniformity

for all samples was greater than 4, indicating that PNF was poorly graded. Coefficient of gradation was in the range of 1–3, indicating that PNF consists of particles of uniform size. Mass-relative span was less than 1, indicating narrow size distribution. The aforementioned results indicate that the variation of particle size in the PNF samples was very less and particles sizes were close to mean value. This confirms particle-size reduction to desirable values. When the size distribution within the samples was compared, it was found that standard geometric deviation is less in HM 1.2. Similar observation was recorded when graphic standard deviation values of each sample were compared. These results indicate that coarser particles were uniformly distributed than fine particles.

Energy consumption in grinding

Impact-type size-reduction equipment presents many advantages compared with others as these machines can finely grind a variety of materials¹⁵. A majority of total power is consumed to move the mechanical parts of the grinding machine (to overcome the friction between the crushing heads, which also contributes to noise as well as heat and vibration losses), and thus, only a small fraction of power (approximately 1%) is actually available for size reduction of material^{16,17}. Therefore, to verify the energy laws, the gross energy required for grinding PNF was considered. The effective energy consumption (kwhr/tonne per reduction ratio) is calculated as follows

Effective energy consumption

$$= \frac{\text{Specific energy consumed (kwhr/tonne)}}{\text{Reduction ratio}}, \tag{17}$$

where reduction ratio is the ratio of initial particle size to the final particle size. The effective energy consumption

Table 6. Energy constants for the three different PNF samples obtained from hammer mill

Grinding equipment (screen)	Rittinger's constant (kWh/tonne mm)	Kick's constant (kWh/tonne)	Bonds constant (kWh/tonne mm ^{0.5})	Work index (kWh/tonne)	Reduction ratio (b)	Specific energy (kWh/tonne) (a)	Effective energy (kWh/tonne)/reduction ratio ((a)/(b))	Mass mean diameter (µm)
HM 1.2	51	39	79	25	3.260	127	38	388.040
HM 0.8	122	97	239	758	3.316	320	96	367.320
HM 0.4	220	179	439	1390	3.359	0.602	179	351.930

Table 7. Raw material and energy requirement to produce one tonne of desirable size of PNF

Hammer mill sieve	Y (cumulative mass fraction) (%)	Raw material required (neem + dolomite 1 : 1) for 1 tonne of PNF (tonne)	Neem fruit required for 1 tonne of PNF (tonne)	Energy required (kWh/tonne)
HM 1.2	29.5	3.389	1.69	213.45
HM 0.8	38	2.631	1.315	395.25
HM 0.4	65	1.53	0.76	412.00

for HM 1.2, HM 0.8 and HM 0.4 was 38, 96 and 179 respectively. Reduction ratio increases with decrease in H_{ss} and more energy is required to grind smaller particles. Rittinger's, Kick's and Bond's constants are listed in Table 6. Regression of experimental energy data to all the three energy laws indicated that the Rittinger's law best fit to PNF grinding ($R^2 = 0.998$).

Application of model in PNF manufacturing

Optimum particle size, based on physiochemical characteristic of PNF, was found to be $\leq 355 \mu\text{m}$ (40 mesh) as reported earlier¹⁰ which is also close to the average size of $390 \mu\text{m}$ obtained from HM 0.4. Therefore to manufacture 1 tonne of PNF of uniform size of $\leq 390 \mu\text{m}$, the amount of whole neem fruit required is calculated using best-fit size distribution model, in this case Rosin–Rammler–Bennett (RRB) model. Using RRB model constants x_R (constant for size parameter) and n_R (constant for distribution parameter) were computed which were used to determine the amount of raw material (whole neem fruit) for the production of 1 tonne of PNF ($\leq 390 \mu\text{m}$) can be determined.

Further energy requirement for production of 1 tonne PNF was computed using Rittinger's law as it was best fit to PNF grinding. Table 7 shows the raw material and energy requirement to produce one tonne of desirable size of PNF. Sample calculation for material and energy requirement corresponding to hammer mill screen HM 0.4 are shown. The cumulative mass fraction is given by equation

$$Y = 1 - \exp[-(x/x_R)^{n_R}], \quad (18)$$

where $x = 390 \mu\text{m}$, $x_R = 464.83$, $n_R = 2.390$ (Table 3) corresponding to HM – 0.4

$$Y = 0.65 \text{ (mass fraction 0.65; mass percentage 65\%)}$$

It means if 1 kg raw material is pulverized then 0.65 kg material has particle size $\leq 390 \mu\text{m}$. Hence to produce 1 tonne of above size PNF the amount of raw neem fruit required

$$= \frac{10000}{0.65} = 1521.21 \text{ kg,}$$

$$= 1.53 \text{ tonne (1.53/2 (neem fruit))}$$

$$+ 1.53/2 \text{ (dolomite))}$$

As the raw material consists of neem fruit and dolomite in 1 : 1 proportion it means 1 tonne of PNF has 500 kg each of neem fruit powder and dolomite.

Therefore the energy required for grinding 0.765 tonne (1.92/2) of whole neem fruit which would yield 1 tonne of PNF ($\leq 390 \mu\text{m}$) by using Rittinger's size reduction law can be computed as

$$E = mK_R[(1/D_p) - (1/D_f)],$$

$$K_R = 220 \text{ (kWh/tonne.mm) (from Table 4)}$$

$$m = 1.22 \text{ tonne}$$

$$E = 0.76 \times 220 [(1/0.390) - (1/10.122)],$$

$$E = 412 \text{ kWh/tonne.}$$

Therefore for one tonne of desired size ($\leq 390 \mu\text{m}$) of PNF energy requirement using hammer mill screen HM 0.4 will be 412 kWh.

Conclusions

Developing a simple method for manufacturing PNF could improve the overall effectiveness as well as reduce

manufacturing cost. At the same time, it is important to verify the quality of PNF from time to time during manufacture. Three common mathematical models were used to study the particle-size distribution of PNF samples, and it was found that the RRB equation has the best fit for particle-size distribution over the entire range of cumulative weight fraction with a high value of coefficient of determination. Application of energy laws showed that energy consumption decreases with increase in hammer mill sieve size. In addition, reduction ratio was found to be very high for lower hammer mill sieve size. The variation of particle size in the PNF samples was very less, and particles sizes were close to mean value. The value of uniformity index UI was >20 and <60 for all samples, which indicates even spreading of PNF.

Based on the calculations it was observed that, to produce 1 tonne of uniformed size PNF 0.76 tonne of neem fruit and 412 kWh/tonne of energy is required.

1. Subbalakshmi, L., Muthukrishnan, P. and Jeyaraman, S., Neem product and their agricultural applications. *J. Biopestic.*, 2012, **5**, 72–76.
2. Verkerk, R. H. J. and Write, D. J., Biological activity of neem seed kernel extract and synthetic azadirachtin against larvae of *Plutellaxystellia* L. *Pestic. Sci.*, 1993, **37**, 83–91.
3. Benjawan, C. P., Chutichudet, S. and Kasewsit. Effect of dolomite application on plant growth. *Int. J. Agric. Res.*, 2010, **5**(9), 690–707.
4. Chen, G. C., He, Z. L., Stoffella, P. J., Yang, X. E., Yu, S. and Calvert, D., Use of Dolomite Phosphate Rock (DPR) fertilizers to reduce phosphorus leaching from sandy soil. *Environ. Pollut.*, 2006, **139**, 176–182.
5. Krishna Murthy, T. P. and Balaraman, M., Grinding studies of mango Ginger: mathematical modeling of particle size distribution and energy consumption. *Food Sci. Technol.*, 2013, **4**, 70–76.
6. Shashidhar, M. G., Krishna Murthy, T. P., Ghiwari, K. and Monohar. B., Grinding of coriander seeds: modeling of particle size distribution and energy studies. *Int. J. Partic. Sci. Technol.*, 2013, **31**(5), 449–457.
7. Macias-Garcia, A., Eduardo, M., Cuerda-Correa and Diaz-Diez, M. A., Application of the Rosin–Rammler and Gates–Gaudin–Schuhmann models to the particle size distribution analysis of agglomerated cork. *Mater. Character.*, 2004, **52**, 159–164.
8. Mohd Rozalli, N. H., Chin, N. L. and Yusol, Y. A., Grinding characteristics of Asian originated peanuts and specific energy consumption during ultra-high speed grinding for natural peanuts butter production. *J. Feed Eng.*, 2015, **152**, 1–7.
9. Miao, Z., Grift, T. E., Hansen, A. C. and Ting, K. C., Energy requirement for comminution of biomass in relation to particle physical properties. *Ind. Crops Prod.*, 2011, **33**, 504–513.
10. Sonali, T., Praful, D., Sayaji, M. and Sachin, M., Characterization and testing of fine powder formulation of whole neem fruits. *Curr. Sci.* (in press).
11. Rosin, P. and Rammler, E., Law governing the fineness of powder coal. *J. Inst. Fuel*, 1993, **7**, 29–36.
12. Harris, C. C., The application of size distribution equation to multi-event comminution process. *Transac. Sem/AIME*, 1986, **241**, 343–358.
13. Folk, R. L. and Ward, W. C., Brazos River Bar. A study on significance of grain size parameters. *J. Sediment. Petrol.*, 1957, **27**, 3–26.
14. Schumann, R., Size distribution and surface calculations, Technical publication no. 1187, Merican Institute of Mining and Metallurgical Engineering, New York.
15. Scholten, R. L. and McElhiney, R. R., The effect of pre breaking in hammer mill particle size reduction, American Society of Agricultural Engineers, St Joseph, MI, 1985, 85–3542.
16. Ghorbani, Z., Masoumi, A. A. and Hemmat, A., Specific energy consumption for reducing the size of alpha chops using a hammer mill. *Biosyst. Eng.*, 2010, **105**, 34–40.
17. Hiremath, R. S. and Kulkarni, A. P., *Unit Operations of Chemical Engineering*, Everest Publishing House, 2011.
18. Canadian Fertilizer Institute, *The CFI Guide of Material Selection for the Production of Quality Blends*, Ottawa, Ontario, Canada, CFL, 2001.
19. Craig, R. F., *Craig's Soil Mechanics*, Spon Press, London, 2004.
20. Hinds, W. C., *Properties, Behaviors and Measurement of Airborne Particles*, Aerosol Technology, John Wiley and Sons, New York, 1992.
21. Allais, I., Edoura-Gaena, R., Gros, J. and Trystram, G., Influence of egg type, pressure and mode of incorporation on density and bubble distribution of a lady finger batter. *J. Feed Eng.*, 2006, **74**, 198–210.

ACKNOWLEDGEMENTS. The authors thank the Board of Research in Nuclear Sciences (2012/35/38/BRNS), Department of Atomic Energy, Government of India, for funding this research.

Received 22 June 2016; revised accepted 10 April 2017

doi: 10.18520/cs/v113/i05/911-918